
Trajectory Model of Occupants Ejected in Rollover Crashes

James R. Funk

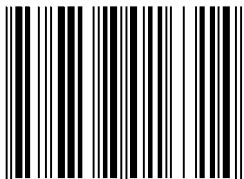
Biodynamic Research Corporation

Peter A. Luepke

Exponent Failure Analysis Associates

Reprinted From: **Accident Reconstruction 2007**
(SP-2063)

ISBN 0-7680-1631-2



9 780768 016314

SAE *International*[™]

2007 World Congress
Detroit, Michigan
April 16-19, 2007

By mandate of the Engineering Meetings Board, this paper has been approved for SAE publication upon completion of a peer review process by a minimum of three (3) industry experts under the supervision of the session organizer.

All rights reserved. No part of this publication may be reproduced, stored in a retrieval system, or transmitted, in any form or by any means, electronic, mechanical, photocopying, recording, or otherwise, without the prior written permission of SAE.

For permission and licensing requests contact:

SAE Permissions
400 Commonwealth Drive
Warrendale, PA 15096-0001-USA
Email: permissions@sae.org
Fax: 724-776-3036
Tel: 724-772-4028



For multiple print copies contact:

SAE Customer Service
Tel: 877-606-7323 (inside USA and Canada)
Tel: 724-776-4970 (outside USA)
Fax: 724-776-0790
Email: CustomerService@sae.org

ISSN 0148-7191

Copyright © 2007 SAE International

Positions and opinions advanced in this paper are those of the author(s) and not necessarily those of SAE. The author is solely responsible for the content of the paper. A process is available by which discussions will be printed with the paper if it is published in SAE Transactions.

Persons wishing to submit papers to be considered for presentation or publication by SAE should send the manuscript or a 300 word abstract of a proposed manuscript to: Secretary, Engineering Meetings Board, SAE.

Printed in USA

Trajectory Model of Occupants Ejected in Rollover Crashes

James R. Funk

Biodynamic Research Corporation

Peter A. Luepke

Exponent Failure Analysis Associates

Copyright © 2007 SAE International

ABSTRACT

A simple two-dimensional particle model was developed to predict the airborne trajectory, landing point, tumbling distance, and rest position of an occupant ejected in a rollover crash. The ejected occupant was modeled as a projectile that was launched tangentially at a given radius from the center of gravity of the vehicle. The landing and tumbling phases of the ejection were modeled assuming a constant coefficient of friction between the occupant and the ground. Model parameters were optimized based on a dolly rollover test of a 1998 Ford Expedition in which five unbelted anthropomorphic test devices (ATDs) were completely ejected. A generalized vehicle dynamics model was also created assuming a constant translational deceleration and a prescribed roll rate function. Predictions using the generalized model were validated against the results of the full-scale rollover test to estimate the expected error when using the model in a real world situation. The model was shown to be a useful tool for investigating possible ejection points and occupant trajectories in rollover crashes.

INTRODUCTION

In spite of increasing seatbelt use, occupant ejection in rollover crashes remains a significant source of injury and death. Ejected occupants comprise half of the more than 9,000 fatalities that occur due to rollover crashes each year (NHTSA, 1997). Over 30% of unbelted occupants involved in rollover crashes are completely ejected (NHTSA, 1997; Parenteau et al., 2001), and 50% of those individuals are seriously injured (Digges and Eigen, 2003). Ejected occupants are five to eight times more likely to be killed in a rollover crash than occupants who remain in the vehicle (Malliaris and Digges, 1987).

In cases of rollovers with ejections, crash investigators are often asked through which portal a particular occupant was ejected and at what point in the rollover event that ejection occurred. To answer these questions, an analysis of the occupant's trajectory from the point of ejection to the point of rest may be helpful. A thorough analysis of the occupant's trajectory requires

the investigator to calculate a range of likely values for the speed and angle of the ejection and the landing, the height and distance associated with the occupant's airborne trajectory, the location of the landing point, and the distance the occupant subsequently tumbled to rest.

There is typically very little information available to the investigator to determine the precise trajectory of an occupant ejected in a rollover crash. The final rest position of an occupant is often recorded in the police report or described by witnesses. Many times, the occupant's ejection portal can be determined based on witness marks on the vehicle and/or knowledge of the occupant's seating position (although in some cases the dispute centers on where the occupant was seated). Only rarely is there obvious forensic evidence indicating at what point in the rollover sequence an occupant was ejected, the height of the airborne trajectory, or the exact location where the occupant landed before sliding to rest. A mathematical model of the post-ejection trajectory would be a useful tool for analyzing possible ejection scenarios.

After reviewing the literature, we are aware of no published model describing the trajectory of occupants ejected in rollover crashes. However, a relevant model describing the trajectory of a pedestrian after being struck by a vehicle was developed by Searle and Searle (1983) using elementary equations of particle motion. The airborne phase of motion was described by a ballistic trajectory. The effect of air resistance was neglected, which was shown by Aronberg (1989) to result in only small errors. Searle (1993) experimentally confirmed that the pedestrian experiences a significant horizontal velocity change upon landing, which is theoretically equal to the coefficient of friction multiplied by the vertical landing velocity, and in reality is somewhat less than that. Searle and Searle (1983) also presented equations demonstrating that an occupant who bounces and tumbles to rest after landing experiences the same average deceleration as an occupant who slides to rest without bouncing, thus providing a theoretical basis for modeling the motion of the pedestrian after landing as frictional. Later research has continued to use the Searle model to analyze the trajectory of pedestrians after they have become airborne

(Wood, 1991). In the present study, a simple two-dimensional model of a rolling and sliding vehicle is developed to predict the speed and angle of an occupant upon ejection, and the Searle model is then used to describe the subsequent trajectory of the occupant traveling through the air, landing on the ground, and tumbling to rest. The model parameters were validated based on a full-scale vehicle dolly rollover test conducted by Exponent Failure Analysis Associates in which five (5) unbelted dummies were fully ejected.

METHODS

GENERALIZED VEHICLE DYNAMICS MODEL

A simplified two-dimensional model of a rolling and sliding vehicle was developed to characterize the kinematics of an occupant being ejected from the vehicle. Several parameters determined from the crash reconstruction are required as inputs to the model. These include the vehicle velocity at the initiation of the rollover (v_{init}), the roll distance (d_{roll}), and an assumed drag factor (f_d) over the known roll distance, which are related to each other according to eq. (1):

$$v_{init} = \sqrt{2f_d d_{roll}} \quad (1)$$

The elapsed time from the initiation of the rollover until rest (t_{roll}) is determined by eq. (2):

$$t_{roll} = \frac{v_{init}}{f_d} \quad (2)$$

Consistent with eq. (1), the horizontal motion of the center of gravity of the vehicle (v_{cg}) is modeled assuming a constant rate of deceleration (f_d) applied over time (t):

$$v_{cg} = v_{init} - f_d t \quad (3)$$

The position of the center of gravity of the vehicle (x_{cg}) relative to the rollover initiation point at any given time (t) is given by:

$$x_{cg} = v_{init} t - \frac{f_d t^2}{2} \quad (4)$$

The vehicle is assumed to roll about its longitudinal axis like a barrel over the ground, with no vertical motion of the center of gravity of the vehicle. Motion about the yaw and pitch axes of the vehicle are also neglected. The roll rate of the vehicle (ω) at each time point is generally unknown in a real world crash. For the purpose of developing a generalized vehicle dynamics model, an equation form was developed that generally matched roll rate vs. time plots measured in various vehicle rollover tests (Orlowski et al., 1985; Thomas et al., 1989;

Cooperrider et al., 1998; Carter et al., 2002; Luepke et al., 2007):

$$\omega(t) = 4\omega_{max} \left(\sqrt{\frac{t}{t_{roll}}} - \frac{t}{t_{roll}} \right) \quad (5)$$

where ω_{max} is the peak roll rate. The roll angle (θ) as a function of time is calculated by integrating the roll rate function:

$$\theta(t) = 4\omega_{max} \left(\frac{2t^{3/2}}{3\sqrt{t_{roll}}} - \frac{t^2}{2t_{roll}} \right) \quad (6)$$

Of course, other equation forms for the roll rate function could be prescribed. Whatever form is chosen for the roll rate vs. time curve, it is necessary that the area under the curve equal the total roll angle (θ_{roll}) as determined by the number of rolls in the event. For the roll rate shape given in eq. (5), the peak roll rate (ω_{max}) is determined by solving eq. (6) for $t = t_{roll}$:

$$\omega_{max} = \frac{3\theta_{roll}}{2t_{roll}} \quad (7)$$

The roll rate as a function of time is therefore given by eq. (5) using the value for ω_{max} determined from eq. (7). The centripetal acceleration (a_{cent}) necessary to keep the occupant inside the vehicle in a curved path having a radius (r) can also be determined at each time point:

$$a_{cent} = \omega^2 r \quad (8)$$

OCCUPANT EJECTION MODEL

In order to determine the path of an ejected occupant, a ballistic trajectory is calculated based on the location and velocity of the occupant at the point of ejection. A coordinate system is established with its origin on the ground below the vehicle's center of gravity at the time of roll initiation (Fig. 1). The x-axis points in the direction of vehicle travel, and the z-axis points up. The location of the occupant at the point of ejection is defined by the position of the vehicle's center of gravity (x_{cg}), the roll angle of the vehicle (θ), and the location of the occupant's portal of ejection with respect to the lateral axis of the vehicle (ϕ):

$$x_{launch} = x_{cg} - r \cos(\theta + \phi) \quad (9)$$

$$z_{launch} = r[1 + \sin(\theta + \phi)] \quad (10)$$

where nominal values for ϕ are 35° for an occupant loaded by the lower portion of the window opening and ejected through the trailing side window and 130° for an occupant loaded by the roof rail and ejected through the leading side window (Fig. 1). The sum of the vehicle roll

angle and the ejection portal angle ($\theta + \phi$) represents the release angle for the occupant. A “slingshot release” is assumed, meaning that the occupant’s launch velocity vector is equivalent to the velocity of the vehicle perimeter at some effective launch radius (r) near the ejection portal. The launch radius is nominally the distance from the center of gravity to the perimeter of the vehicle. Distances of 41 in. between the center of gravity and the beltline and 48 in. between the center of gravity and roof rail were calculated from measurements of an exemplar 1999 Ford Expedition (Fig. 1).

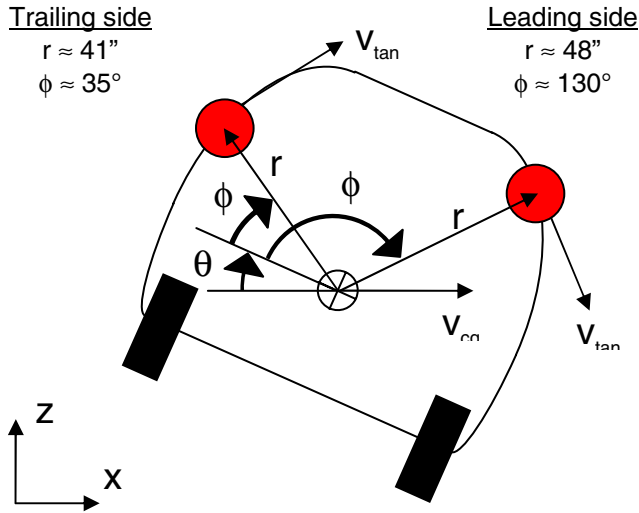


Figure 1. Illustration depicting various parameters of the occupant ejection model. Occupants are modeled as particles shown here as circles on the vehicle perimeter. Nominal values for launch radius (r) and ejection portal angle (ϕ) are given for a 1998 Ford Expedition.

The launch velocity vector is given by the vector sum of the longitudinal velocity of the center of gravity of the vehicle and the tangential velocity of the occupant at the ejection portal:

$$v_{x_launch} = v_{cg} + \omega r \sin(\theta + \phi) \quad (11)$$

$$v_{z_launch} = \omega r \cos(\theta + \phi) \quad (12)$$

The airborne trajectory of the ejected occupant is then calculated assuming that the rollover event occurred on a flat surface. First, the maximum height (h_{max}) attained by the ejected occupant is calculated:

$$h_{max} = z_{launch} + \frac{v_{z_launch}^2}{2g} \quad (13)$$

where g is the acceleration due to gravity (32.2 ft/s²). This maximum height is only attained by an occupant who is ejected with an upward component to their launch velocity vector. If an occupant is ejected downward ($v_{z_launch} < 0$), then h_{max} represents the equivalent fall height of the occupant’s trajectory. The vertical component of the landing velocity is calculated from h_{max} :

$$v_{z_land} = \sqrt{2gh_{max}} \quad (14)$$

Air resistance is neglected, and the horizontal component of the landing velocity is assumed to be the same as the horizontal component of the launch velocity:

$$v_{x_land} = v_{x_launch} \quad (15)$$

The time spent in the air (t_{air}) is equal to the time going up to the maximum height plus the time falling down to the ground:

$$t_{air} = \frac{v_{z_launch}}{g} + \sqrt{\frac{2h_{max}}{g}} \quad (16)$$

This equation is valid even if the launch trajectory is downward ($v_{z_launch} < 0$). The distance the ejected occupant is thrown through the air (d_{throw}) is then:

$$d_{throw} = v_{x_launch} t_{air} \quad (17)$$

and the landing location (x_{land}) is:

$$x_{land} = x_{launch} + d_{throw} \quad (18)$$

Upon impact with the ground, the occupant’s vertical velocity drops to zero. Impact with the ground also results in a corresponding loss of horizontal velocity (Δv_{x_land}) due to frictional forces acting during impact (Searle and Searle, 1983):

$$\Delta v_{x_land} = \mu_{slide} v_{z_land} \quad (19)$$

where μ_{slide} is the sliding coefficient of friction between the occupant and the ground. Of course, Δv_{x_land} cannot be greater than v_{x_land} .

The distance that an ejected occupant tumbles or slides (d_{slide}) after hitting the ground can be determined by the residual horizontal velocity of the occupant after the ground impact and the sliding friction coefficient:

$$d_{slide} = \frac{(v_{x_land} - \mu_{slide} v_{z_land})^2}{2\mu_{slide} g} \quad (20)$$

The rest position of the occupant (x_{rest}) is therefore:

$$x_{rest} = x_{land} + d_{slide} \quad (21)$$

The occupant ejection model was implemented in the form of an Excel spreadsheet that calculated the occupant trajectory up to final rest for hypothetical ejections occurring at various time points throughout the rollover sequence. Possible points of ejection were determined by matching the rest position of the occupant

calculated by the model (eq. 21) to the actual documented rest position of the occupant.

MODEL PARAMETER OPTIMIZATION

Optimized values for the launch radius (r) and the sliding coefficient of friction between the occupant and the ground (μ_{slide}) were determined based on the trajectories of five anthropomorphic test devices (ATDs) ejected in a vehicle dolly rollover test described in a companion paper (Luepke et al., 2007). The test vehicle was a 1998 Ford Expedition in which the tempered glass in the side door and rear quarter panel windows had been removed and replaced with laminated glass. The vehicle was instrumented with angular rate sensors about the roll and yaw axes. Six (6) Hybrid II 50th percentile male ATDs were seated in the vehicle in the left and right outboard seating positions of the first, second, and third row seats. Their seating positions were designated by row and side (i.e., 1L, 1R, 2L, 2R, 3L, and 3R). None of the ATDs were restrained. The vehicle was placed in an FMVSS 208 rollover dolly in a driver's side leading configuration. The speed of the dolly was 43.2 mph at contact with the snubber tubes, which rapidly decelerate the dolly and initiate the rollover. The vehicle traveled approximately 120 feet over packed soil and completed four (4) rolls, coming to rest on its wheels. Five of the ATDs were ejected. The crash was captured with high speed digital video (250 Hz frame rate) from several on-board and off-board cameras. Post-crash scene evidence, including the rest positions of the dummies, was measured and photographed.

A detailed analysis of the dolly rollover test was performed (Luepke et al., 2007). The time history of the translational velocity of the center of gravity of the vehicle was calculated based on the location of physical evidence and analysis of the high speed video data. Time histories for roll angle and roll rate were calculated from the roll rate sensor. The experimentally obtained time histories were compared to the generalized vehicle dynamics model (eq.'s 3 and 5). Times and positions are reported with the zero point corresponding to the end of the initial tire marks.

The occupant ejection model was validated using the accident reconstruction data from the test (Luepke et al., 2007) combined with a trajectory analysis of each ejected dummy. The time, vehicle position, and occupant position were determined for the points of ejection and ground contact based on analysis of the high speed digital video and the physical evidence. The time of occupant ejection could only be determined approximately from the video, since the entire ejection process occurred over approximately a quarter of a second and involved ATD interaction with a variety of vehicle structures. The exact time of ejection was chosen based on the "slingshot release" assumption so that the predicted trajectory of the dummy matched the observed trajectory. At this time point, the ATD was approximately halfway out of the window opening. It was possible to determine the location

of landing for all of the ejected ATDs from photographs of disturbances in the ground. The time of landing was defined as the moment when the center of gravity of the dummy struck the ground in the video.

Combining standard equations of motion, the maximum height (h_{max}) was then determined for each ejected occupant:

$$h_{\text{max}} = z_{\text{launch}} + \frac{g}{2} \left(\frac{t_{\text{air}}}{2} - \frac{z_{\text{launch}}}{gt_{\text{air}}} \right)^2 \quad (22)$$

The horizontal ($v_{x_{\text{launch}}}$) and vertical ($v_{z_{\text{launch}}}$) components of the launch velocity were then calculated:

$$v_{x_{\text{launch}}} = \frac{d_{\text{throw}}}{t_{\text{air}}} \quad (23)$$

$$v_{z_{\text{launch}}} = \pm \sqrt{2g(h_{\text{max}} - z_{\text{launch}})} \quad (24)$$

where the sign of $v_{z_{\text{launch}}}$ was positive for an upward trajectory and negative for a downward trajectory. The horizontal ($v_{x_{\text{land}}}$) and vertical ($v_{z_{\text{land}}}$) components of the landing velocity were calculated using eq. (15) and eq. (14), respectively. Lastly, the coefficient of sliding friction (μ_{slide}) between the occupant and the ground was calculated for each dummy ejection by solving eq. (20) using the quadratic formula:

$$\mu_{\text{slide}} = \frac{v_{x_{\text{land}}} v_{z_{\text{land}}} + gd_{\text{slide}} - \sqrt{gd_{\text{slide}}(2v_{x_{\text{land}}} v_{z_{\text{land}}} + gd_{\text{slide}})}}{v_{z_{\text{land}}}^2} \quad (25)$$

The launch radius (r) was estimated for each ejected ATD by using the occupant ejection model with reconstructed rollover test data to match the trajectory as determined above. Because all of the model parameters were interrelated, the value for the launch radius had to be optimized in an iterative fashion until the model results matched the experimental data with minimal error.

MODEL VALIDATION

The occupant ejection model was additionally validated in combination with the generalized vehicle dynamics model to simulate the real world situation in which there is no high speed video of the rollover crash and only very basic reconstruction parameters and the occupant rest position are known. Ranges for the ejection model parameters were determined based on the results of the present study (Table 1). For each occupant, eight versions of the combined generalized vehicle dynamics and occupant ejection model were created, corresponding to all possible combinations of the high and low ends of the ranges for vehicle drag factor (f_d), occupant launch radius (r), and occupant sliding coefficient of friction (μ_{slide}). Possible ejection points and

their associated trajectories as predicted by the model were compared to the experimental data. Most models predicted several possible points of ejection at various stages of the rollover sequence that matched the rest position of the dummy. Of course, only one of these predicted ejection scenarios can be accurate. For the purpose of validating the model, results are only listed for the possible point of ejection corresponding most closely to the time of actual ejection in the test. This validation tests, therefore, only assess the accuracy of the model when predicting the true ejection scenario.

Table 1. Input parameters for model validation.

Generalized vehicle dynamics model	
Roll distance (d_{roll})	106 ft
Number of rolls (θ_{roll})	4 rolls (1440°)
Vehicle drag factor (f_d)	0.3 – 0.5
Occupant ejection model	
Leading side occupant	
Launch radius (r):	48 – 54 in.
Ejection portal angle (ϕ):	130°
Trailing side occupant	
Launch radius (r):	41 – 47 in.
Ejection portal angle (ϕ):	35°
Occupant sliding drag factor (μ_{slide})	0.5 – 0.7

RESULTS

DOLLY ROLLOVER TEST

Five out of the six ATDs were fully ejected from the vehicle during the rollover. One ATD (2L) remained in the vehicle. Three of the ATDs were ejected on the “high” side, meaning that they left the vehicle with an initially upward trajectory (occupants 1L, 1R, and 2R). All of these ATDs landed and slid to rest well beyond the vehicle’s final point of rest (Figure 2). Two of the ATDs

were ejected on the “low” side, meaning that they left the vehicle with an initially downward trajectory (occupants 3L and 3R). Both of these ATDs were initially thrown ahead of the vehicle and then rolled over by the vehicle. Dummy 3L was pushed forward when its back was struck by the top left rear corner of the vehicle, which then rolled over it. Dummy 3R was actually hit twice by the rolling vehicle. After its initial bounce off the ground, it was hit in the face by the left rear bumper. Then the vehicle rolled over its pelvis, leaving an indentation in the left roof rail between the C and D pillars. In all of the ejections, there was a forward component to the tangential velocity vector. In other words, all of the ejections occurred at a release angle ($\theta + \phi$) between 0° and 180°. There were no “deposits” in which the dummy was ejected at a low speed near the ground. All of the dummies experienced high energy impacts upon landing, with landing velocities ranging from 38 – 48 mph and landing angles ranging from 23° – 46° (Table 2). Four of the ejected ATDs landed from an equivalent maximum height of 10 – 14 feet, and the other ATD (1R) was launched to a height of 31 feet. In all of the ejected ATDs, body parts became detached due to landing: the left leg of dummy 1L, the left hand of dummy 1R, the pelvic insert of dummy 2R, the left arm of dummy 3L, and the pelvic insert and right arm of dummy 3R.

MODEL PARAMETER OPTIMIZATION

Optimized friction coefficients and launch radii were calculated for each of the five ejected ATDs based on an analysis of the high speed video, the physical evidence on the ground, the reconstructed velocity time history of the vehicle (Figure 3), and the measured roll rate of the vehicle (Figure 4) (Luepke et al., 2007). Values for the friction coefficient and launch radius could be optimized so that the model matched the test data almost exactly (most errors < 1 ft, 1 mph, and 1 deg).

Table 2. Summary of results. Positions are relative to the trip point, defined as the end of the initial tire marks.

ATD seating position	1L	3L	1R	2R	3R
Vehicle speed at ejection (mph)	22 mph	20 mph	28 mph	20 mph	28 mph
Vehicle position at ejection (ft)	50 ft	55 ft	26 ft	55 ft	37 ft
Throw distance (ft)	100 ft	14 ft	117 ft	77 ft	16 ft
Slide distance (ft)	44 ft	20 ft	4 ft	13 ft	11 ft
ATD rest position (ft)	191 ft	91 ft	143 ft	142 ft	66 ft
Equivalent maximum height (ft)	14 ft	10 ft	31 ft	14 ft	12 ft
Roll number at ejection	1.76	1.97	0.91	1.98	1.27
Roll rate at ejection (deg/s)	467 deg/s	441 deg/s	525 deg/s	440 deg/s	510 deg/s
Revised for 1R			615 deg/s		
Launch velocity (mph)	45 mph	42 mph	41 mph	36 mph	46 mph
Launch angle (deg)	19 deg	-16 deg	45 deg	27 deg	-17 deg
Landing velocity (mph)	47 mph	44 mph	42 mph	38 mph	48 mph
Landing angle (deg)	26 deg	23 deg	46 deg	33 deg	24 deg
Time in air (s)	1.62 s	0.24 s	2.71 s	1.66 s	0.25 s
Launch radius (in)	52 in	48 in	55 in	46 in	41 in
Revised for 1R			48 in		
Sliding coefficient of friction	0.56	0.95	0.67	0.73	1.24
Body region of primary impact	Head	Right side	Head	Left side	Right side

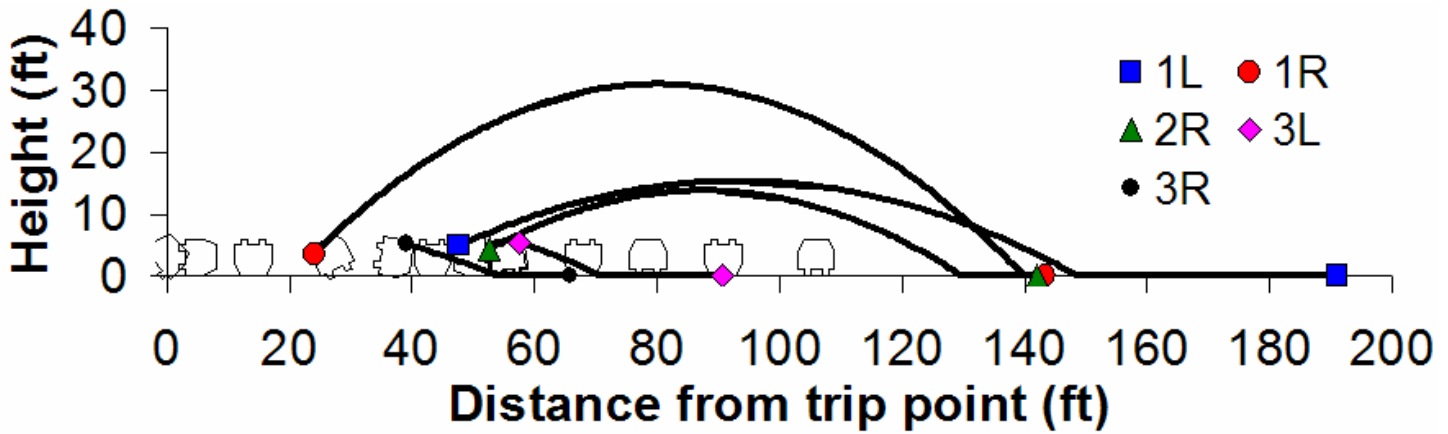


Figure 2. Illustration of the trajectories of the five dummies ejected in the dolly rollover test.

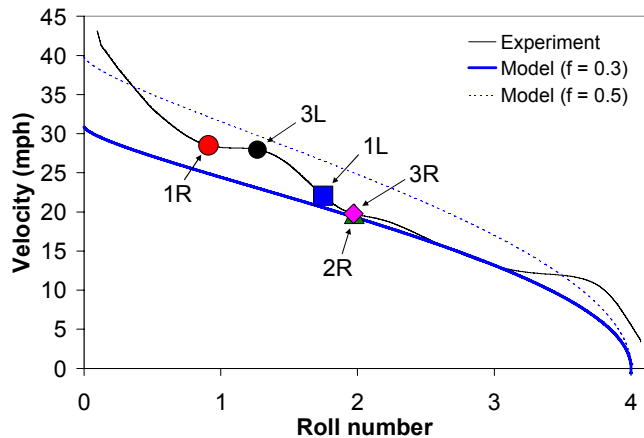


Figure 3. Translational vehicle velocity vs. roll number for the dolly rollover test (Luepke et al., 2007) and generalized vehicle dynamics model. Ejection points for each dummy are shown on the experimental curve.

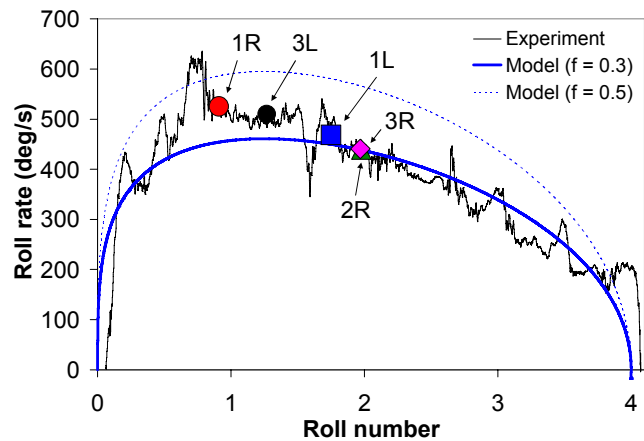


Figure 4. Roll rate vs. roll number for the dolly rollover test (Luepke et al., 2007) and generalized vehicle dynamics model. Ejection points for each dummy are shown on the experimental curve.

The calculated friction coefficient for the dummy sliding on the ground ranged from 0.56 – 1.24 (Table 2). However, the friction coefficient calculated for dummies 3L and 3R was considered questionable, because both dummies were rolled over by the vehicle before they had

come to rest. The average friction coefficient for the remaining three ATDs was 0.66, which is in good agreement with the literature (Wood and Simms, 2000).

The estimated launch radii for the five ejected ATDs ranged from 41 – 52 in. In most cases, the estimated launch radius was slightly greater (up to 7 in.) than the nominal distance between the center of gravity and the perimeter of the vehicle as measured on an exemplar (Figure 5). In the case of dummy 1R, the estimated launch radius of 55 in. seemed unrealistically high. It was observed that the roll rate had plateaued for a time at approximately 615 deg/s just prior to the estimated ejection point, but then had dropped to 525 deg/s at the estimated time of ejection (Figure 4). A revised estimate of the launch radius for dummy 1R was determined using a roll rate was 615 deg/s (Table 2). This revised estimate was 48 in., which was 7 in. higher than the distance between the center of gravity and the undeformed beltline of the right front door (Fig. 1).

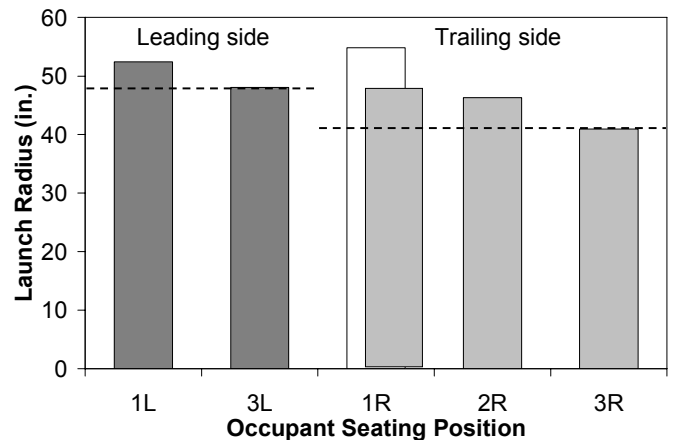


Figure 5. Estimated launch radii. Nominal values (see Fig. 1) are shown as dashed lines. For dummy 1R, the original estimate is shown as a white bar, and the revised estimate is shown as a gray bar.

MODEL VALIDATION

The generalized vehicle dynamics model reasonably approximated the experimental data. However, in

contrast to the model, the test vehicle did not decelerate at a constant rate. Rather, the vehicle experienced a sharp loss in velocity initially, followed by decelerations that varied from approximately 0 – 1 g as the vehicle tumbled along the ground (Luepke et al., 2007). The range of vehicle velocities predicted by the range of drag factors chosen for study (0.3 – 0.5) reasonably approximated the actual vehicle velocity (Figure 3). The roll rate calculated using the prescribed function in eq. (5) bracketed most of the test data over the range of interest, but underestimated the peak roll rate (Figure 4).

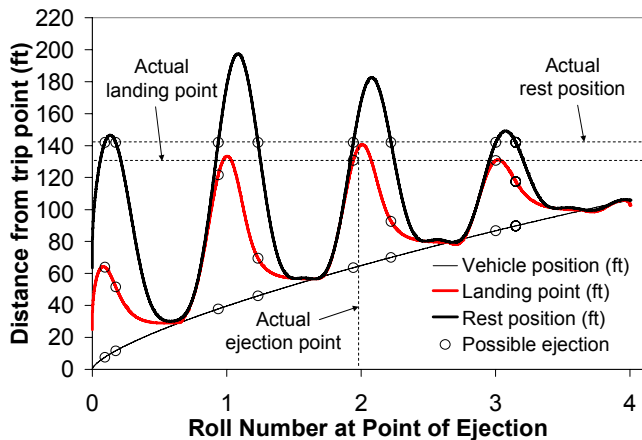


Figure 6. Sample simulation of combined generalized vehicle dynamics model and occupant ejection model for dummy 2R. The model predicts eight possible ejection scenarios, one of which closely approximates the actual ejection scenario observed in the full-scale rollover test.

Table 3. Validation results for generalized vehicle dynamics model combined with occupant ejection model using the range of parameters given in Table 1.

		Throw dist (ft)	Equiv max height (ft)	Roll # at ejection
1L	Actual	100	14	1.76
	Predicted	77 - 136	12 - 38	1.65 - 1.80
3L	Actual	14	10	1.97
	Predicted	5 - 10	16 - 34	2.04 - 2.11
1R	Actual	117	31	0.91
	Predicted	80 - 108	13 - 28	0.87 - 1.01
2R	Actual	77	14	1.98
	Predicted	64 - 84	12 - 27	1.88 - 2.01
3R	Actual	16	12	1.27
	Predicted	3 - 6	15 - 30	1.36 - 1.43

When the occupant ejection model was combined with the generalized vehicle dynamics model, there were 4 – 8 possible ejection scenarios for each occupant that matched the final rest position of the occupant (Figure 6). Occupants had up to two opportunities per vehicle roll to get ejected and end up at a given point of rest. They could either be launched high into the air and slide a short distance or they could be launched downward and slide a longer distance. For purposes of model validation in this study, only the ejection scenario most closely

corresponding to the actual ejection scenario was evaluated. Over the range of input parameters studied (Table 1), the range of trajectories predicted by the combined generalized vehicle dynamics and occupant ejection model usually encompassed or came close to the actual values from the dolly rollover test (Table 3). The range of predicted throw distances (and by extension, slide distances) was fairly wide. The range of predicted ejection heights was extremely wide. However, the range of predicted ejection points was fairly narrow, and it appeared that if a particular ejection scenario could be verified, the model could usually predict the roll angle of the vehicle at the time of ejection to within approximately 30°.

DISCUSSION

The trajectory of occupants ejected in rollover crashes can be analyzed with reasonable accuracy using a simple model and basic physics equations. The trajectory model presented here includes many simplifying assumptions that require validation. First, the model was two-dimensional, and ignored the effects of vehicle yaw. As expected, this assumption did not lead to errors when the model was validated against a lateral dolly rollover test. In cases with significant yaw, this assumption should be reevaluated. Second, the model neglected vertical motion due to pitch or bouncing of the rolling vehicle. Interestingly, although there was noticeable vertical motion of the vehicle in the test, the model predictions were nonetheless accurate. Third, the ejected occupant was modeled as a particle that was instantaneously released as if from a slingshot. In actuality, the ejected ATD was a large, articulating mass that took roughly a quarter of a second to completely pass through the ejection portal. However, at some point, the ATD reached free flight, and its trajectory could be traced back to a single, discrete point where the vector sum of the vehicle’s translational and tangential velocity vectors accurately predicted the trajectory of that free flight. This “point” of ejection had physical significance because it defined the ejection trajectory. It corresponded to the time when the body of the ATD was approximately halfway through the window opening, validating the assumption that the occupant could be modeled as a particle that was loaded by the perimeter of the vehicle through its center of gravity at the time of ejection. The “point” of ejection defined in the present study occurred before the ATDs were fully ejected as defined by Luepke et al. (2007).

Although some of the calculated launch radii appeared to be somewhat greater than the nominal values measured in an undeformed vehicle, these differences can be explained to some extent by vehicle deformation that occurred during the rollover. The launch radii calculated for the ejected ATDs 1R and 2R were 6 – 7 in. greater than the nominal values measured in an undeformed

vehicle (Figure 5). The ATDs in these seating positions were on the trailing side of the vehicle and were therefore loaded by the beltline of the door when ejected. Substantial deformation of the doors, particularly the right front door, due to occupant loading from the centrifugal force of the rollover was observed on video. Analysis of the ejection of dummy 1R initially predicted a launch radius of 54 in., which implied 13 in. of outward deformation of the door. This amount of deformation appeared unrealistically high, and it was felt that the high tangential velocity of dummy 1R at the point of ejection was more likely due to the higher roll rate of 615 deg/s that the ATD was experiencing during the process of being ejected. Therefore, the estimate of the launch radius was revised to reflect that higher roll rate, and the revised estimate of 47 in. seemed more reasonable. The launch radii for the other three ATDs were within 4 in. of the nominal values measured in an underformed vehicle. The ATDs in these seating positions were either loaded by the roof rail (1L and 3L) or the bottom of a fixed window frame in which there was no door (3R). Less deformation was observed for those structures, and the calculated launch radii more closely matched the nominal values measured in an undeformed vehicle.

The nature of the glazing in the window openings through which the ejections occurred was not felt to have any effect on the trajectory of the ejected ATDs. By the time the occupant has reached the "point" of ejection as defined in this paper, his or her body is halfway through the window opening, and the glazing is no longer resisting the motion of the occupant. At that point, the occupant is being loaded by edge of the window opening (not the glazing), and the launch vector is defined by the vector sum of the translation velocity of the vehicle and the tangential velocity of the relevant portion of the vehicle perimeter. Therefore, the occupant ejection model is felt to be valid whether the window opening was previously occupied by laminated glass, tempered glass, or even no glass (i.e., the window was down).

Although the assumptions of the occupant ejection model were well validated by the dolly rollover test, the assumptions of the generalized vehicle dynamics model were less accurate. Notably, the vehicle in the dolly rollover test did not decelerate at a constant rate, as is often assumed in rollover reconstructions (Figure 3). Instead, the vehicle experienced alternating periods of high deceleration during ground contacts and low deceleration during airborne phases.

In addition to the error introduced by the assumption of constant vehicle deceleration, some consideration should be given to the error introduced by assuming a prescribed roll rate function, given the variation in the shape of measured roll rate vs. time curves (Orlowski et al., 1985; Thomas et al., 1989; Cooperrider et al., 1998; Carter et al., 2002; Luepke et al., 2007). It is also recognized that the model assumes an initial roll angle of zero, when in actuality a rolling vehicle will already have

rolled some amount (approximately 45 degrees) before the leading tires stop leaving marks. This assumption simplified the calculations, and was found to create error only in the very early part of the roll sequence (Figure 4). The prescribed roll rate function suggested in eq. (5) is a smooth curve with a peak roll rate that is only 1.5 times the average roll rate (eq. 7). It was found to generally match the measured roll rate over the region of interest (Figure 4). However, it was less accurate during the beginning and ending of the event, and it underpredicted the peak roll rate in this test.

The generalized vehicle dynamics model represents the least accurate crash reconstruction, because it utilizes the minimum amount of information necessary to reconstruct a rollover crash. In real world cases, it is often possible to determine average velocities and roll rates over various portions of the rollover sequence based on matching physical evidence on the vehicle and the ground, and this specific information can be used to refine the vehicle dynamics model. The more specific the vehicle dynamics model can become as a result of additional detail in the crash reconstruction, the more accurate the predictions of the occupant ejection model will be.

Perhaps the most important limitation of the entire model is that in most cases in which a vehicle has rolled multiple times, the model predicts several possible points of ejection, and the model by itself cannot determine which of those possible ejection scenarios is most likely. It is up to the investigator to combine the model results with other evidence to determine the most likely ejection scenario(s) through a process of elimination. For example, the model often predicts possible ejections before the vehicle has even rolled one quarter turn. These possibilities can usually be excluded as unrealistic. In addition, possible ejection points prior to glass breakage can usually be excluded. If the rolling vehicle followed a curving path, the possible points of ejection can be narrowed down by analyzing the expected direction of ejection at various points in the roll sequence in relation to the final rest position of the occupant. Occasionally, obstacles in the path of a possible ejection trajectory may be used to exclude that ejection scenario as a possibility. The nature of an ejected occupant's injuries may also provide clues as to whether the occupant experienced a severe landing and/or slid a long distance.

The model validation exercise employed in this study demonstrated that with a good crash reconstruction, the occupant ejection model can achieve good accuracy. In general, the model can estimate roll angles at the point of ejection within a narrow range. The height and throw distance associated with the ejection trajectory can also be predicted, but over a much wider range. The model predictions are most sensitive to errors in the roll rate and launch radius, and least sensitive to errors in the value of the sliding coefficient of friction between the

occupant and the ground. The sliding friction parameter is of only minor importance unless its value is very small or very large. Results of the model as it was validated in this paper should be interpreted as defining a range of probable ejection scenarios. To bracket all or nearly all possible ejection scenarios would require a wider range of input parameters than those studied here (Table 1).

The purpose of the present study was to establish a theoretical model for analyzing the trajectories of occupants ejected in rollover crashes and to determine preliminary values for the model parameters. Although informative, the results from the present study only reflect a single crash test, and cannot be considered a statistically significant sample. It is hoped that in the future, this simple model can be further validated against additional vehicle rollover tests, and possibly with real world crashes captured on video. Extending the equations to handle changes in the elevation of the terrain would also be useful.

CONCLUSIONS

A simple two-dimensional particle model for analyzing occupant ejections in rollover crashes was developed. The model with optimized parameters was shown to accurately predict the kinematics of five ejected ATDs in a vehicle dolly rollover test. The results demonstrated that at the point of ejection, the ATDs assumed the resultant velocity of the portion of the vehicle perimeter against which they were loading. The landing and sliding phases of the ejection were accurately modeled by simple friction. This mathematical tool can be used to investigate possible ejection scenarios in a real world case if the rest position of the occupant is known and crash reconstruction information is available. Additional analysis using other physical evidence is typically required to determine which of several ejection scenarios most likely occurred in a given crash.

ACKNOWLEDGMENTS

We gratefully acknowledge Ford Motor Company for funding the full-scale rollover test and Richard Morrison, Glass & Glazing Forensics, Inc. for coordinating the design and fabrication of the laminated glass.

REFERENCES

1. National Highway Traffic Safety Administration, "Analysis of Ejection in Fatal Crashes," Research Note, November 1997.
2. Parenteau, C., Gopal, M., Viano, D., "Near and Far-Side Adult Front Passenger Kinematics in a Vehicle Rollover," Paper 2001-01-0176, *Society of Automotive Engineers*, 2001.
3. Digges, K.H. and Eigen, A.M., "Crash Attributes that Influence the Severity of Rollover Crashes," Paper 231, *Proc 18th Enhanced Safety of Vehicles*, 2003.

4. Malliaris, A.C. and Digges, K.H., "Crash Protection Offered by Safety Belts," *Proc 11th Enhanced Safety of Vehicles*, Washington, D.C., 1987.
5. Searle, J.A. and Searle, A., "The Trajectories of Pedestrians, Motorcycles, Motorcyclists, etc., Following a Road Accident," Paper 831622, *Society of Automotive Engineers*, pp. 277 – 285, 1983.
6. Aronberg, R., "Airborne Trajectory Analysis Derivation for Use in Accident Reconstruction," Paper 900367, *Society of Automotive Engineers*, pp. 135 – 142, 1990.
7. Searle, J.A., "The Physics of Throw Distance in Accident Reconstruction," Paper 930659, *Society of Automotive Engineers*, pp. 71 – 81, 1993.
8. Wood, D.P., "Application of a Pedestrian Impact Model to the Determination of Impact Speed," Paper 910814, *Society of Automotive Engineers*, pp. 121 – 157, 1991.
9. Orłowski, K.F., Bundorf, R.T., Moffatt, E.A., "Rollover Crash Tests – The Influence of Roof Strength on Injury Mechanics," Paper 851734, *Proc. 29th Stapp Car Crash Conference*, pp. 181 – 203, 1985.
10. Thomas, T.M., Cooperrider, N.K., Hammoud, S.A., Woley, P.F., "Real World Rollovers – A Crash Test Procedure and Vehicle Kinematics," *Proc. 12th International Conference on the Enhanced Safety of Vehicles (ESV)*, pp. 819 – 825, 1989.
11. Cooperrider, N.K., Hammoud, S.A., Colwell, J., "Characteristics of Soil-Tripped Rollovers," Paper 980022, *Society of Automotive Engineers*, pp. 51 – 59, 1998.
12. Carter, J.W., Habberstad, J.L., Croteau, J., "A Comparison of the Controlled Rollover Impact System (CRIS) with the J2114 Rollover Dolly," Paper 2002-01-0694, *Society of Automotive Engineers*, 2002.
13. Luepke, P., Carhart, M., Croteau, J., Morrison, R., Loibl, J., Ridenour, J., "An Evaluation of Laminated Side Window Glass Performance During Rollover," Paper 2007-01-0367, *Society of Automotive Engineers*, 2007.
14. Wood, D. and Simms, C., "Coefficient of Friction in Pedestrian Throw," *Impact*, 9(1): 12 – 15, 2000.

CONTACT

James R. Funk
Biodynamic Research Corporation
5711 University Heights Blvd., Suite 100
San Antonio, TX 78249
Phone: 210-691-0281
Fax: 210-691-8823
E-mail: jfunk@brconline.com